Journal of Cell Science 112, 4243-4255 (1999)
Printed in Great Britain © The Company of Biologists Limited 1999
JCS0914

E-MAP-115 (ensconsin) associates dynamically with microtubules in vivo and is not a physiological modulator of microtubule dynamics

Kathleen Faire[1], Clare M. Waterman-Storer[2,3], Dorota Gruber[1], Danièle Masson[4], E. D. Salmon[2] and J. Chloë Bulinski[1,*]

[1]Departments of Anatomy & Cell Biology and Pathology, Columbia University, College of Physicians & Surgeons, 630 W. 168th St, Rm BB1213, New York, NY 10032-3702, USA
[2]Department of Biology, CB3280, 607 Fordham Hall, University of North Carolina, Chapel Hill, NC, 27599, USA
[3]Department of Cell Biology, Scripps Research Institute, 10550 Torrey Pines Rd, La Jolla, CA 92037, USA
[4]Laboratoire Réseau Epithélium, Centre Médical Universitaire, 1, rue Michel-Servet, CH-1211 Genève 4, Switzerland
*Author for correspondence (e-mail: jcb4@columbia.edu)

Accepted 28 September; published on WWW 17 November 1999

SUMMARY

Microtubule-associated proteins (MAPs) have been hypothesized to regulate microtubule dynamics and/or functions. To test hypotheses concerning E-MAP-115 (ensconsin) function, we prepared stable cell lines expressing conjugates in which the full-length MAP (Ensc) or its microtubule-binding domain (EMTB) was conjugated to one or more green fluorescent protein (GFP) molecules. Because both distribution and microtubule-binding properties of GFP-Ensc, GFP-EMTB, and 2×, 3×, or 4×GFP-EMTB chimeras all appeared to be identical to those of endogenous E-MAP-115 (ensconsin), we used the 2×GFP-EMTB molecule as a reporter for the behavior and microtubule-binding function of endogenous MAP. Dual wavelength time-lapse fluorescence imaging of 2×GFP-EMTB in cells microinjected with labeled tubulin revealed that this GFP-MAP chimera associated with the lattice of all microtubules immediately upon polymerization and dissociated concomitant with depolymerization, suggesting that dynamics of MAP:microtubule interactions were at least as rapid as tubulin:microtubule dynamics in the polymerization reaction. Presence of both GFP-EMTB chimeras and endogenous E-MAP-115 (ensconsin) along apparently all cellular microtubules at all cell cycle stages suggested that the MAP might function in modulating stability or dynamics of microtubules, a capability shown previously in transiently transfected cells. Although cells with extremely high expression levels of GFP-EMTB chimera exhibited stabilized microtubules, cells expressing four to ten times the physiological level of endogenous MAP exhibited microtubule dynamics indistinguishable from those of untransfected cells. This result shows that E-MAP-115 (ensconsin) is unlikely to function as a microtubule stabilizer in vivo. Instead, this MAP most likely serves to modulate microtubule functions or interactions with other cytoskeletal elements.

Key words: Fluorescent speckle microscopy, Taxol, Carcinoma cell, Non-motor MAP

INTRODUCTION

Cells elaborate characteristic assemblies of microtubules (MTs) to carry out cell motility, transport and positioning of vesicles and organelles, segregation of chromosomes, and alteration and maintenance of cell morphology. Elucidating mechanisms that govern the spatial and temporal distribution and the dynamics of MTs is critical to understanding MT function in growing and differentiating cells.

Although properties intrinsic to the tubulin dimer define the physical behavior of MTs, this behavior is also influenced by differential expression of tubulin isotypes, post-translational modifications, and interactions with MT-associated proteins (MAPs) (Ludueña, 1998). MAPs identified based upon their affinity for MTs, but not for tubulin dimer, include the tau, MAP1, and MAP2 families, which are found predominantly or exclusively in nervous tissue (Matus, 1988). These MAPs have been shown to promote MT assembly, both in vitro and in vivo (Mandelkow and Mandelkow, 1995).

In non-neuronal cells and tissues, other MAPs decorate the MT wall. Two of these, MAP4 and a MAP that has been called 125K MAP, E-MAP-115, or ensconsin, were originally isolated from the cervical carcinoma line, HeLa (Bulinski and Borisy, 1979; Weatherbee et al., 1980). While MAP4 has been shown to stabilize and modulate the level of MTs in vivo (e.g. Nguyen et al., 1999), studies performed to date have not determined in vivo functions of E-MAP-115 (ensconsin).

In vitro studies and expression in transiently transfected cells have shown that E-MAP-115 (ensconsin) is a basic protein of ~84 kDa with aberrant electrophoretic mobility, a single N-terminal MT-binding domain lacking homology to other MAPs (Masson and Kreis, 1993), and biochemical properties distinct from other MAPs (Bulinski and Bossler, 1994). Notably, E-

MAP-115 (ensconsin) is altered in MT-binding in the presence of the MT-stabilizing drug, taxol (Bulinski and Bossler, 1994), and it does not compete with MAP4 for binding to MTs (Bulinski and Borisy, 1980).

E-MAP-115 (ensconsin) was bound to and shown to stabilize MTs in transiently transfected cells (Masson and Kreis, 1993) and under certain in vitro conditions (Bulinski and Bossler, 1994). By immunofluorescence the MAP co-localized with MTs in cultured cells; either showing heterogeneous labeling that diminished toward the cell periphery (Masson and Kreis, 1993), or uniform labeling throughout the MT network (Bulinski and Bossler, 1994). In mitotic cells, immunofluorescence and sedimentation demonstrated release of the MAP from MTs at the onset of mitosis, coincident with increased phosphorylation (Masson and Kreis, 1995). These results gave rise to the hypothesis that E-MAP-115 (ensconsin) modulates MT dynamics or stability in vivo and that this function is, in turn, modulated during the cell cycle.

Expression data also provided correlative evidence evocative of E-MAP-115 (ensconsin) functions. For example, abundant expression during mouse epithelial development seemed consistent with a role in differentiation or maintenance of epithelia (Fabré-Jonca et al., 1998). The facts that the MAP's expression level was shown to increase during epithelial differentiation (Masson and Kreis, 1993; Fabré-Jonca et al., 1999), and that MTs were found to acquire enhanced stability concurrently (Bre et al., 1990; Pepperkok et al., 1990), suggested that this MAP might contribute, at least in part, to MT stabilization during epithelial differentiation. These data elevated the plausibility of the hypothesis that E-MAP-115 (ensconsin) functions as a MT-stabilizing protein in vivo.

Although its expression has been correlated with differentiation, E-MAP-115 (ensconsin) is also prominently expressed in HeLa and MCF-7 carcinoma cells, and less abundantly in other cell lines. Though epithelial in origin, these cell lines do not show polarity, adhesion, or migratory properties characteristic of differentiated epithelial cells (Bulinski and Bossler, 1994), and they do not possess unusual MT stability. However, they represent a useful model in which to test the hypothesis that E-MAP-115 (ensconsin) functions to stabilize MTs in vivo. Studies described here make use of cells stably expressing the full-length MAP or its MT-binding domain, conjugated to GFP(s). We show here that GFP-MAP chimeras faithfully mimic all MT-binding behaviors of endogenous MAP and elucidate the dynamic association of E-MAP-115 (ensconsin) with all cellular MTs at all cell cycle stages. Surprisingly, results of detailed analyses of the dynamics of individual MTs in cells expressing GFP-MAP chimera are inconsistent with the hypothesis that E-MAP-115 (ensconsin) modulates MT dynamics in an in vivo context.

MATERIALS AND METHODS

Materials

Except as noted, chemicals were from Sigma (St Louis, MO) or Fisher Scientific (Tustin, CA), tissue culture supplies, lipofectamine, and oligonucleotides were from Gibco Life Sciences (Gaithersburg, MD), restriction enzymes were from Promega Biotech (Madison, WI) or New England Biolabs (Beverly, MA), and immunochemicals were from Organon Technika (Malvern, PA).

Preparation of GFP-ensconsin constructs

Using oligonucleotide primers (Table 1), we amplified fragments of cDNA clones encoding portions of E-MAP-115 (ensconsin) and GFP, generating plasmids encoding GFP conjugated to either full-length MAP (GFP-Ensc) or its MT-binding domain (GFP-EMTB). All primers contained restriction sites for insertion into the plasmid, and novel sites for cloning or verifying constructs (Table 1). Conditions for all PCR reactions used in making GFP chimeras were as follows:

Table 1. Oligonucleotide primers used in the preparation of GFP conjugates

	Oligonucleotide primer sequence	Corresponding nucleotide position
GFP-Ensc primers		
5′	ATAAAGCTTATGGAGCAGAAGCTCATCTCAGAAGAAGACCTCGGCGCGCCAGTGC GAAGCGAAACA	152-166 (E-MAP-115)
3′	GCTGTGTCGGATCCCCATCTA	2309-2329 (E-MAP-115)
GFP-EMTB primers		
5′	ATAAAGCTTATGGAGCAGAAGCTCATCTCAGAAGAAGACCTCGGCGCGCCAGTG CGAAGCGAAACA	152-166 (E-MAP-115)
3′	ATATGGATCCGAAGAGCCCTCAGGTGG	932-9552 (E-MAP-115)
2×GFP-EMTB primers		
5′	ATAAAGCTTATGGAGCAGAAGCTC	152-166 (E-MAP-115)
3′	ATATCCGCGGTCCACTTCCCTTGTACAGCTCGTC	1381-1400 (GFP)
3×GFP-EMTB primers		
5′	ATATCCGCGGGATATCCCTGAGGGCTCTTCG	935-949 (E-MAP-115)
3′	ATATCCGCGGGGTACCGCGGCCGCTTTCCTTGTA	1390-1407 (GFP)
4×GFP-EMTB primers		
5′	ATATCCGCGGGATATCCCTGAGGGCTCTTCG	935-949 (E-MAP-115)
3′	ATATCCGCGGGATATCCTTGTACAGCTC	1384-1396 (GFP)

Sequences and corresponding nucleotide position of oligonucleotide primers used in PCR reactions to generate the GFP-chimeras. The nucleotide positions listed correspond to sequences posted in GenBank under accession numbers U55762 (for pEGFP-N1) and X73882 (for E-MAP-115). Restriction enzyme sites indicated in underlined type were included in each primer in order to facilitate insertion of the PCR product into the construct and to aid in subsequent sequence verification.

94°C for 30 seconds, 50°C for 30 seconds, 72°C for 1 minute, for a total of 30 cycles. For all GFP-chimeras, PCR products excised from agarose gels, were purified with Geneclean (Bio 101, Vista, CA) and ligated into applicable sites in the appropriate plasmid.

The plasmid, pGFP-Ensc, was made by PCR, using full-length E-MAP-115 cDNA as template (Masson and Kreis, 1993) and primers shown in Table 1. To prepare pGFP-EMTB, we used a partial length human cDNA as PCR template; the same 5′ primer as for pGFP-Ensc was paired with a different 3′ primer. PCR products for pGFP-Ensc and pGFP-EMTB were cloned into *Hin*dIII and *Bam*HI sites of pEGFP-N1 (Clontech, Inc., Palo Alto, CA). Preparation of plasmids encoding EMTB conjugated to GFP multimers (2×, 3×, and 4×GFP-EMTB) was similar in strategy: PCR products obtained using pGFP-EMTB as template and primers listed in Table 1 were cloned into naive pEGFP-N1, p2×GFP-EMTB, and p3×GFP-EMTB, yielding p2×GFP-EMTB, p3×GFP-EMTB and p4×GFP-EMTB, respectively.

To verify constructs, we sequenced each newly created junction by digesting plasmids with BsiHKAI, purifying the ~720 bp fragments obtained, blunt-ending them with T4 DNA polymerase, and subcloning them into the *Sma*I site of pBluescript. We identified fragments with appropriate junctions by checking for the presence of a restriction site unique to each. Each fragment was sequenced with T7 and T3 promoters, using a T7 Sequenase, Version 2.0 Sequencing Kit (U.S. Biochemical, Cleveland, OH).

Preparation of stable cell lines expressing GFP chimeric proteins

TC-7 or MCF-7 cells were transfected with pGFP-Ensc, pGFP-EMTB, p2×-, p3×-, and p4×-GFP-EMTB, or with pGFP-MAP4-MTB (Nguyen et al., 1999). Efficiency of transfections, performed as described by Nguyen et al. (1999) except using 15 μl lipofectamine, was assessed microscopically after 36-48 hours. Cells were selected with geneticin (G418) for 3 weeks to generate stable lines, then colonies were isolated with cloning cylinders (Bellco, Inc., Vineland, NJ), and tested for expression by immunofluorescence and quantitative western blotting. In some cases, transfectants were sorted via FACS, 72 hours after transfection (as described by Nguyen et al., 1999), and either plated for cloning, or analyzed immediately.

Immunological analysis

Polyclonal anti-EMTB antibodies raised in guinea pigs by Pocono Farms (Canadensis, PA) against 6×-his-tagged EMTB expressed from pRSETA-EMTB, were used at a 1/2000 dilution for quantitative immunoblot analysis, which was performed as described (Chapin and Bulinski, 1991a). Quantification of GFP-EMTB chimera expression and tubulin content was performed using extracts of HeLa cells and naive TC-7 cells as standards, since abundance of E-MAP-115 (ensconsin) and tubulin in these extracts had been determined previously (Bulinski and Borisy, 1979; Chapin and Bulinski, 1991b). The ratio (mol EMTB chimera: mol tubulin) was used to calculate number of EMTB chimeric molecules per micron of MT, assuming that MAP chimeras and tubulin partitioned alike between monomeric and polymeric pools.

Immunofluorescence was performed as described by Bulinski and Bossler (1994), except using image capture and manipulation procedures described by Nguyen et al. (1997). As noted elsewhere, in some experiments cells were extracted (4 minutes, 37°C) in 80 mM Pipes, pH 6.8, 5 mM EGTA, 1 mM $MgCl_2$, 0.5% Triton-X 100, before fixation. The fluorescence localization of GFP-MAP chimeras resembled immunofluorescence results obtained in TC-7 cells with either anti-EMTB antibody or anti-ensconsin antibody (Bulinski and Bossler, 1994); only slight differences were observed that were attributable to differences between weaker and stronger anti-MAP antibody reactivity.

Two different procedures were used to measure mitotic index: First, to compare naive TC-7 cells with those expressing EMTB chimeras, cells from log phase cultures were fixed in methanol and stained with DAPI and anti-tubulin; cells with mitotic figures were scored as a proportion of total cells. Fixation and staining steps often depleted cultures of some less adherent mitotic cells; therefore, mitotic indices of cell lines were always compared within a single experiment. Second, to compare TC-7 transfectants with each other, rather than with naive cells, mitotic index was scored using GFP fluorescence to identify mitotic cells; we confirmed that each cell with mitotic chromosomes contained a GFP-labeled spindle.

Imaging of MTs in living transfected cells

TC-7 cells plated on glass coverslips were imaged as described by Waterman-Storer and Salmon (1997). For analysis of drug-treated cells, each coverslip was placed in a custom-designed perfusion chamber (Waterman-Storer and Salmon, 1998b), and medium with or without nocodazole was introduced. Dual time-lapse imaging and processing of images were performed as described by Waterman-Storer and Salmon (1997). MT dynamics were quantified in naive TC-7 cells or in stable transfectants expressing GFP-MAP chimeras, as described by Waterman-Storer and Salmon (1997). Briefly, cells on glass coverslips were microinjected with porcine brain tubulin labeled with X-rhodamine succinimidyl ester (Molecular Probes, Eugene, OR). They were imaged with a Nikon 60× PlanApochromat objective (NA, 1.4), 1-1.5× optivar, and a Hammamatsu C4880 cooled CCD camera, using a digital multi-mode imaging system, controlled by Metamorph software (Universal Imaging Corp., West Chester, PA) (all described by Salmon et al., 1998). Time-lapse images were collected at intervals of 3-15 seconds; for all experiments described here, a 10 or 15 second interval was used. For dual-wavelength imaging of X-rhodamine and GFP-EMTB, images were captured 1.5 seconds apart from one another, and 1 second exposures were used for both red and green images. Parameters of MT dynamics were determined by tracking positions of MT ends over time, using the 'TrackPoints' function of Metamorph. Velocities of growth and shortening were determined using RTM custom software (Walker et al., 1988) as described (Waterman-Storer and Salmon, 1997). *P* values were obtained from raw data for each MT, using the *t*-test (not paired) function of SigmaPlot (Jandel Scientific, San Rafael, CA).

RESULTS

GFP-MAP chimeric proteins bind to MTs when expressed in stable cell lines

To test hypotheses concerning in vivo functions of E-MAP-115 (ensconsin), we prepared stable transfectants of African green monkey kidney cells, TC-7, and human breast carcinoma cells, MCF-7, expressing chimeric proteins comprised of GFP conjugated to the C terminus of either the full-length MAP (GFP-Ensc; e.g. Fig. 1a,c) or its MT-binding domain (GFP-EMTB; Fig. 1b,d). We cloned stable cell lines for each because it was necessary or desirable to analyze cell populations whose content of GFP chimera was as uniform and constant as possible, during more than ten passages in culture.

Initial observations of live cells expressing GFP-Ensc (GFP-Ensc-TC-7 or -MCF-7 cells) or GFP-EMTB (GFP-EMTB-TC-7 or -MCF-7 cells) revealed fluorescence on cytoplasmic fibers (Fig. 1) whose coincidence with MTs was shown by tubulin immunofluorescence (data not shown). Thus, appending GFP to the C terminus of full-length MAP or EMTB did not compromise its MT binding. In contrast, addition of GFP to the N terminus prevented MT binding of either molecule (data not shown).

In brightly fluorescent cells, e.g. GFP-EMTB-TC-7 or -MCF-7 cells (Fig. 1b,d) we observed GFP-MAP chimera

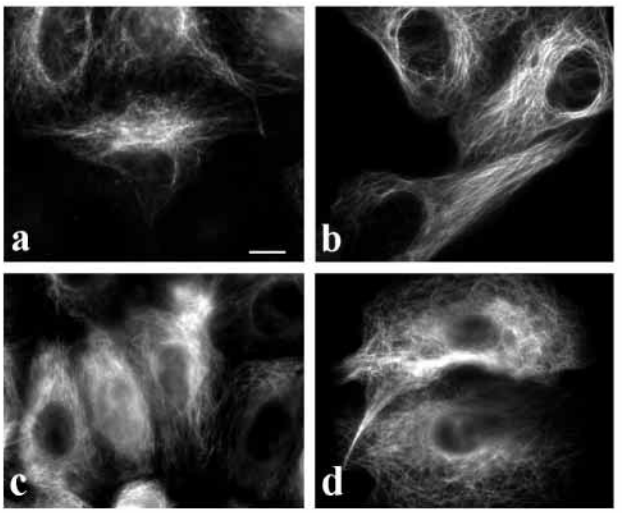

Fig. 1. Distribution of GFP-E-MAP-115 (ensconsin) chimeric proteins in living cells. Images of TC-7 (a) and MCF-7 (c) cells transfected with GFP-Ensc, and TC-7 (b) and MCF-7 (d) cells transfected with GFP-EMTB. Note that all cells show fluorescent MTs that emanate radially from the central region of the cell. Bar, 10 μm.

along the length of all MTs, as they extended from the cell center to the periphery. In more dimly fluorescent cells, such as GFP-Ensc-TC-7 (Fig. 1a) or GFP-Ensc-MCF-7 (Fig. 1c), we noted that fluorescence from MT-bound GFP-MAP chimera often appeared to predominate near the nucleus, because the density of MTs was greater there. In contrast, little or no GFP-Ensc was visible in peripheral regions (see Fig. 1a and c). Western blots (Fig. 2) showed that the level of expression of GFP-MAP chimera was higher in GFP-EMTB cells (Fig. 2b,c) than in GFP-Ensc cells (Fig. 2a), and that level was higher than the level of E-MAP-115 (ensconsin) endogenous to HeLa cells (Fig. 2d). Our results were qualitatively similar for TC-7 and MCF-7 transfectant lines; however, we concentrated our studies on the former, because of their flatter morphology.

Abnormal MT phenotypes have been observed in cells expressing high levels of another MAP, MAP4 (e.g. Olsen et al., 1995; Nguyen et al., 1997; Bulinski et al., 1997). To preclude the possibility of aberrant behaviors in GFP-EMTB transfectants, we prepared TC-7 cells expressing low levels of EMTB conjugated to multiple, rather than a single, GFP molecule. As shown in Table 2, TC-7-EMTB cells expressed 400 molecules of GFP-EMTB per micron of MT, a level that is 11.4 times the level of E-MAP-115 (ensconsin) endogenous to a HeLa cell and 26 times that in a TC-7 cell; this level exceeds the saturating level of MT binding sites (Bulinski and Bossler, 1994). In contrast, cells transfected with EMTB linked to GFP multimers expressed from 10-200 molecules of GFP-MAP chimera per micron of MT. Expression of GFP-MAP chimeras in these cells was quantified on blots such as those shown in Fig. 2, lanes d-i, and reported in Table 2. HeLa cell extracts (e.g. Fig. 2, lanes j-l) were used as standards for comparison, since the level of E-MAP-115 (ensconsin) expressed in this line is well established.

As shown in Fig. 3a-c, the fluorescence intensity was similar in cells expressing 2×, 3×, and 4×GFP-EMTB chimeras. We also noted that photobleaching of the GFP, which is impervious to prevention by anti-oxidants, was less pronounced in cells of these three lines than in either GFP-EMTB- or GFP-Ensc-TC-7 cells. Images in Fig. 3a-c, resemble those in Fig. 1b and d; as noted above, from these bright images it appeared that the GFP-MAP chimera was uniformly distributed along cellular MTs.

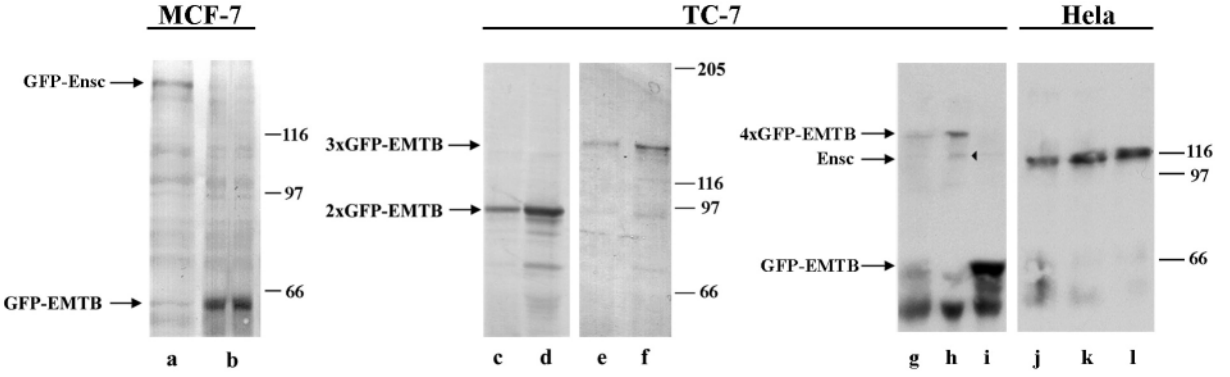

Fig. 2. Expression of GFP-E-MAP-115 (ensconsin) chimeric proteins in clonal cell lines of MCF-7 and TC-7 cells. Western blots of extracts from MCF-7 clonal cell lines a, GFP-Ensc-MCF-7 cells, expressing GFP conjugated to full-length E-MAP-115 (ensconsin); lane b, GFP-EMTB-MCF-7, i.e. GFP conjugated to the MT-binding domain of E-MAP-115 (ensconsin), lanes c-f, TC-7 cells expressing multiple GFPs conjugated to E-MTB. Lanes c, 2×GFP-EMTB-TC-7-L and d, 2×GFP-EMTB-TC-7-H, samples from cells exhibiting low and high level of EMTB conjugated to two GFP molecules, respectively. Lanes e, 3×GFP-EMTB-TC-7-L and f, 3×GFP-EMTB-TC-7-H, samples from cells exhibiting low and high level expression of EMTB conjugated to three GFP molecules. Lanes g, h, samples from 4×GFP-EMTB-TC-7 cells sorted into lower (g) and higher (h) expressing cells via FACS, and i, sample from GFP-EMTB-TC-7. Lanes j-l, samples of HeLa cells included for comparison on the same blot. The band attributed to endogenous E-MAP-115 (ensconsin) band is labeled (Ensc); it is visible in the HeLa samples (lanes j-l), and is marked with an arrowhead in lane h. The bands corresponding to each GFP-chimeric molecule, GFP-Ensc, GFP-EMTB, and 2×, 3×, and 4×GFP-EMTB, are also marked. A species of ~40 kDa that reacts non-specifically with the EMTB antibody used here is visible, especially in those blots reacted via the sensitive technique of ECL (lanes g-l). Blots a-f were developed with chromogenic substrate, 4-chloro-1-naphthol, while blots g-l were developed using ECL. Expression levels of GFP-conjugates are shown in Table 2; approximate amounts of protein electrophoresed in each of the above lanes were the following: a-c, 40 μg; d,e, 15 μg; f, 25 μg; g, 15 μg h, 20 μg; i, 10 μg; j, 30 μg; k, 40 μg; l, 50 μg.

Table 2. Expression of GFP-ensconsin chimeras in clonal transfected cell lines

	Cell type					
GFP-EMTB expression	GFP-EMTB-TC-7	2×GFP-EMTB-TC-7-H	2×GFP-EMTB-TC-7-L	3×GFP-EMTB-TC-7-H	3×GFP-EMTB-TC-7-L	TC-7-4×GFP-EMTB-L
EMTB/total protein (%)	1.64±0.124 (*n*=2)	0.917±0.228 (*n*=6)	0.605±0.137 (*n*=6)	0.302±0.053 (*n*=4)	0.162±0.007 (*n*=4)	<0.1* (*n*=2)
EMTB/MT (molecules/μm MT)	399±30	216±5.0	142±8.4	107±12.5	57.3±1.8	7-32*

All values represent mean ± standard deviation. The number of experiments performed (*n*) is given for each. Molecules per micron MT is calculated from the amount of expression measured, based upon determinations of the abundance of tubulin in all lines of TC-7 cells, the relative molecular masses of tubulin and the MAP, the assumption that E-MAP-115 (ensconsin) and tubulin partition equivalently between the monomeric and polymeric pools, and the calculation that there are 1650 tubulin dimers per micron along a MT.

*Expression was not detectable under the same western blot conditions in which HeLa E-MAP-115 (ensconsin) could easily be detected; more sensitive detection with ECL, rather than the chromogenic substrate used for the highly expressing cell lines revealed a band (Fig. 2g,h) These ECL blots, with HeLa samples as standards, were used to calculate a range of expression in the cultures; however, again the experiment was performed three times. Thus, no error has been calculated for the 4×GFP-EMTB-TC-7 cells, as it was for the other cell types. 4×GFP-EMTB-TC-7 cells express less than the 0.11% (35 mol/μm MT) of endogenous MAP expressed by HeLa cells, and about the same as the 0.03±0.02% *(n*=4*), or* 15 mol/μm MT, expressed by naive TC-7 cells. Note that expression of endogenous E-MAP-115 (ensconsin)-could only be detected via blots developed with ECL.

This impression was verified by examination of high magnification images of 4×GFP-EMTB-TC-7 cells. As shown in Fig. 3d and e, GFP fluorescence in 4×GFP-EMTB-TC-7 cells was resolved into discrete speckles along MTs, instead of continuous fluorescence. From Table 2 we calculate that each fluorescent speckle in Fig. 3d and e, corresponds to a diffraction-limited spot (~240 nm) containing, at most, four molecules of 4×GFP-EMTB. High resolution images of MTs assembled from a tubulin pool containing a low fraction of fluorescently labeled tubulin were previously found to be speckled. These speckles are thought to arise by stochastic incorporation of labeled and unlabeled subunits into MTs (Waterman-Storer and Salmon, 1998a), speckles have been used to analyze movement and dynamics by 'fluorescent speckle microscopy' (Waterman-Storer et al., 1998; Perez et al., 1999). Here, images in which speckle density on subnuclear and peripheral MTs is, in general, roughly equivalent add to the evidence we previously provided from standard immunofluorescence studies (Bulinski and Bossler, 1994); quantification of speckle density yields additional, more quantitative evidence that E-MAP-115 (ensconsin) is not concentrated on particular MTs or in discrete cellular regions, but is uniformly distributed along all cellular MTs.

GFP-EMTB chimeras are faithful reporters for endogenous MAP in phenotypically normal cells

To obtain valid answers to questions about the in vivo behavior of E-MAP-115 (ensconsin), it was vital to demonstrate that cells expressing GFP-MAP conjugates did not show artifactual changes in MT-dependent behaviors. The MT arrays in cells with low expression levels (<150 molecules of GFP-MAP chimera per micron of MT) were normal in morphology, in contrast to cells with very high expression levels, which exhibited bundles of highly stabilized MTs (Table 3). These bundles were morphologically similar to those resulting from transient transfection of E-MAP-115 (ensconsin) constructs (Masson and Kreis, 1993). Since MT abnormalities often result in defects in mitosis, we also measured the mitotic index and incidence of spindle abnormalities (that is, multipolar spindles) in the cell lines (Table 3). Cells expressing low levels of GFP-MAP chimeras were phenotypically normal by this measure, as well.

We also needed to demonstrate that the exogenous GFP-MAP chimeras were identical to endogenous MAP in their MT-binding characteristics. Regardless of fluorescence intensity, in

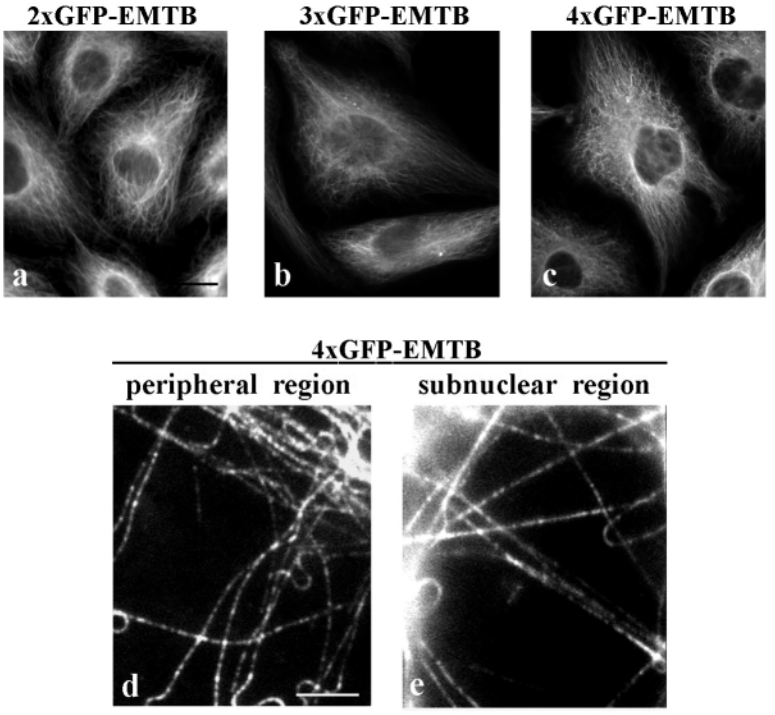

Fig. 3. TC-7 cells expressing multimeric GFP-MAP constructs. (a) 2×GFP-EMTB-TC-7, (b) 3×GFP-EMTB-TC-7, and (c-e) 4×GFP-EMTB-TC-7 cells. Note that MTs in these cells were similar in fluorescence intensity; identical exposure times (1 second) were used to capture images shown in a-c. (d and e) High magnification images of regions near the cell periphery (d, peripheral) and beneath the cell nucleus (e, subnuclear) are shown. Note that MTs in both regions of the cell showed similar fluorescence intensity from the bound 4×GFP-EMTB construct; quantification of speckles that are visible at this high magnification (data not shown) suggests that the density of binding of E-MAP-115 (ensconsin) was similar in the peripheral and subnuclear regions of cells. Bars: in c,10 μm (for a-c); in d, 5 μm (for d and e).

Table 3. Microtubule phenotypes of TC-7 cells expressing GFP-EMTB

(A) Assay of fixed cells, using DAPI and anti-tubulin staining

Cell line	Microtubule bundles?	Mitotic index	Abnormal spindles
Naive TC-7	No	3.9±0.2% (*n*=3)	16% (*n*=118)
GFP-EMTB-TC-7	Yes	8.5±1.5% (*n*=2)	36% (*n*=118)
2×GFP-EMTB-TC-7-L	No	3.2±0.5% (*n*=2)	15% (*n*=130)
3×GFP-EMTB-TC-7-L	No	4.2±0.6% (*n*=2)	8.7% (*n*=183)

(B) Assay of live cells, using GFP fluorescence

Cell line	Microtubule bundles?	Mitotic index	Abnormal spindles
GFP-EMTB-TC-7	Yes	7.3±0.4% (*n*=3)	20% (*n*=35)
2×GFP-EMTB-TC-7-H	Yes	3.9±0.4% (*n*=3)	54% (*n*=31)
2×GFP-EMTB-TC-7-L	No	2.2±0.3% (*n*=2)	0% (*n*=21)
3×GFP-EMTB-TC-7-L	No	2.4±0.9% (*n*=3)	4.7% (*n*=21)

All values represent mean ± standard deviation.

Microtubule bundles were assayed visually; that the bundles were composed of stable MTs was documented by their resistance to breakdown by nocodazole (10 μM, 2 hours, a treatment sufficient to break down all other cellular MTs).

Mitotic index varied due to growth and experimental conditions; therefore, different cell lines were always compared within a single experiment, using a single protocol (DAPI and anti-tubulin staining, or GFP fluorescence in live cells). For determination of mitotic index, the number of experiments (*n*) is indicated for each value; >200 cells were scored to determine each value.

Abnormal spindles were scored as those that were multipolar; the '*n*' given is the total number of metaphase figures examined.

all GFP-EMTB-TC-7 cell lines, the distribution of GFP-MAP chimera faithfully monitored the in vivo localization of endogenous MAP. For example, GFP-MAP chimeras were bound to all cellular MTs and all showed similarly tight binding. Like endogenous E-MAP-115 (ensconsin) (Bulinski and Bossler, 1994), GFP-MAP chimeras remained associated with MTs after detergent lysis and extraction (Fig. 4). The identically exposed micrographs of GFP-Ensc-TC-7 cells before (Fig. 4a) and after (Fig. 4b) detergent extraction show that GFP-Ensc was not released from the MTs by extraction. Identical results were obtained with GFP-EMTB and 2×GFP-EMTB (data not shown). Efficacy of the extraction is shown in Fig. 4c and d, in which a GFP-MAP4 chimera can be seen to be substantially extracted by detergent, in agreement with behavior of endogenous MAP4 (Bulinski and Bossler, 1994).

Identical MT-binding characteristics were also determined quantitatively in vitro; endogenous MAP, GFP-EMTB, and 2×GFP-EMTB partitioned identically when taxol-stabilized MTs were extracted with different salt concentrations, or partially depolymerized with calcium (Bulinski et al., 1999; data not shown). Thus, GFP-EMTB chimeras and endogenous MAP bound equally tightly to cellular MTs; the identical binding properties of these GFP-MTB chimeras permitted their use as authentic reporters of the MAP's in vivo MT-binding behavior, and allowed us to use these reporters to determine how MT dynamics are modulated by bound MAP.

GFP-MAP and endogenous MAP are bound to cellular MTs throughout the cell cycle

Previous immunofluorescence and biochemical assays showed that, in HeLa cells, E-MAP-115 (ensconsin) dissociated from MTs during late G_2, was absent from the primary spindle formed during prophase or from nocodazole-arrested spindles (corresponding to prometaphase figures). The MAP was shown to regain its spindle localization subsequently, becoming completely MT-associated again by the time the cells reached metaphase (Masson and Kreis, 1995). In the cell types we examined, TC-7 and MCF-7, the behavior of either GFP-EMTB (Fig. 5a-h,j) or GFP-Ensc (Fig. 5i) did not appear to corroborate previous findings; both remained associated with MTs throughout the entire cell cycle in TC-7 and MCF-7 cells, notably including late G_2, prophase, and prometaphase stages. Fig. 5 shows that MT localization was observed during M-phase in living cells (a-c,f,i), fixed cells (d,g,j), and cells detergent-extracted and then fixed (e). GFP-EMTB (Fig. 5c) and GFP-Ensc (data not shown) were also associated with abnormal, multipolar spindles, which were frequently found in

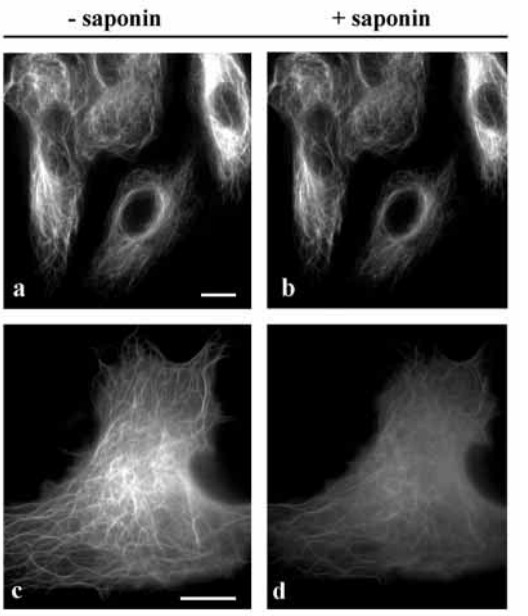

Fig. 4. GFP-E-MAP-115 (ensconsin) chimeric proteins are tightly associated with cytoplasmic MTs. Living TC-7 cells transfected with (a,b) GFP-Ensc or (c,d) GFP-MAP4-MTB, were photographed before (a,c) and after (b,d) perfusion of the slide with 0.2% Saponin in Hepes-buffered, serum-free culture medium for 3 minutes at 37°C, on a heated microscope stage. Note that the GFP-Ensc remained associated with MTs despite detergent extraction (b). In contrast, detergent extracted much of the GFP-MAP4-MTB (d). Results were identical in cells expressing the other GFP-chimeras, GFP-EMTB and 2×GFP-EMTB (data not shown). Bars: in a and c, 10 μm (for a,b and c,d, respectively).

cells abundantly expressing GFP-MAP chimeras (Table 3). Finally, it was striking that endogenous E-MAP-115 (ensconsin), detected by immunofluorescence, showed identical distribution in TC-7 cells (Fig. 5k-o), or in MCF-7 cells (data not shown). These data show that E-MAP-115 (ensconsin) does not dissociate from spindle MTs in either cell line we examined, in contrast to behavior reported in HeLa cells (Masson and Kreis, 1995).

Dynamic association of GFP-MAP chimera with cellular MTs during polymerization/depolymerization

The fact that E-MAP-115 (ensconsin) is bound to the MT array during all cell cycle stages in TC-7 cells catalyzed two questions: First, does each individual MT possess bound MAP? Second, what are the dynamics of the MAP's MT association/dissociation, especially relative to the dynamics of MT polymerization and depolymerization? To address these questions, we used 2×GFP-EMTB-TC-7-L cells, which show normal MT distribution and mitotic properties (Figs 1, 3, 5; Table 3) and express GFP-MAP chimeras that are high fidelity reporters for the MT-binding and localization of the endogenous MAP.

We performed dual wavelength time-lapse digital fluorescence imaging of microinjected X-rhodamine labeled MTs and expressed 2×GFP-EMTB; two sample time points from such a sequence are shown in Fig. 6A,B. Four cells are visible, most notably a yellow (Y) and an orange (O) cell, both of which contain expressed 2×GFP-EMTB and microinjected X-rhodamine tubulin; coincidence of green and red fluorescence at different relative levels yielded yellow or orange fluorescence. Also shown in Fig. 6 are a red cell (R), which expressed a very low level of 2×GFP-EMTB but exhibited red fluorescence from microinjected X-rhodamine tubulin; and a green cell (G), which expressed 2×GFP-EMTB but lacked X-rhodamine tubulin. The yellow cell's MTs showed apparent coincidence of red and green fluorescence all the way to the end of each MT, in every image of the sequence, revealing that all MTs in 2×GFP-EMTB-TC-7-L cells contained bound MAP throughout their lengths, whether they were shrinking, growing or pausing (Fig. 6). In addition, when we determined the positions of the ends of 87 dual-labeled MTs in six TC-7 cells, by comparing X-rhodamine and 2×GFP-EMTB fluorescent images (data not shown), we again detected no MT end devoid of 2×GFP-EMTB label.

As one means of facilitating detection of any MT ends or regions that did not possess bound MAP, we subtracted 2×GFP-EMTB images from X-rhodamine images; the result is shown for the two time points in Fig. 6C and D. We saw no indication of MTs or MT ends lacking bound 2×-GFP-EMTB, although we did note lateral movement of some MTs (Fig. 6, subjacent MTs noted by arrowheads).

To examine this point further, we analyzed the ends of MTs in 2×GFP-EMTB-TC-7-L cells by a technique independent of lateral movements. We generated life-history plots of the ends of red and green MTs, from the sequence excerpted in Fig. 6. In the example shown in Fig. 6E, tracking at intervals separated by 1.5 seconds revealed that at no time did the length change of the MT end, determined from GFP-EMTB and X-rhodamine-tubulin images, differ by more than one micron, a value within our experimental error for MT tracking. These results suggest that the rate that MAP binds to the MT lattice is at least as rapid as the rate of tubulin association to growing ends during steady-state polymer assembly in these cells.

To address the dynamics of MAP association with MTs during de novo polymerization, rather than under steady-state in vivo conditions, we depolymerized all cellular MTs with nocodazole, microinjected cells with X-rhodamine tubulin, and performed a nocodazole washout during dual-wavelength time-lapse fluorescence imaging. In 2×GFP-EMTB-TC-7-L cells in which MTs were depolymerized by nocodazole (0:0. 0 minutes; Fig. 7a) 2×GFP-EMTB fluorescence appeared diffuse, as did X-rhodamine tubulin fluorescence in the same

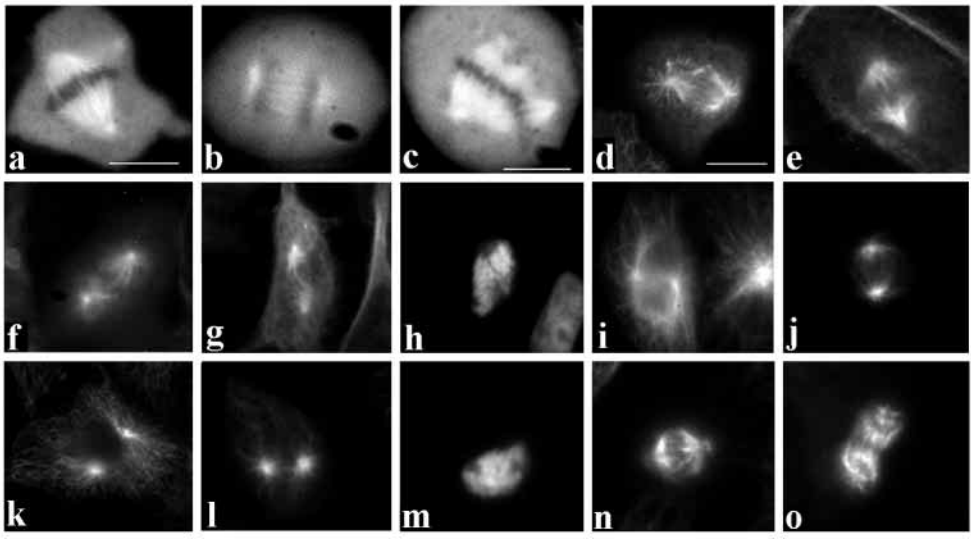

Fig. 5. E-MAP-115 (ensconsin) remains associated with microtubules throughout all stages of mitosis. Images of GFP-EMTB-TC7 cells (a-h), GFP-Ensc-MCF-7 cells, (i), and GFP-EMTB-MCF-7 cells (j), and naive TC-7 cells (k-o) are shown at various cell cycle stages; including metaphase (a,c,e,n), anaphase (b,j,o), prophase (g,l), prometaphase (d,f,) and late G_2 phase (i,k). (a-c,f,i) Living cells; (d,g,h,j) cells fixed in methanol, (e) a cell extracted with detergent and then fixed, (k-o) cells fixed in methanol and stained with anti-ensconsin (Bulinski and Bossler, 1994) or anti-EMTB antibodies (see Materials and Methods), to elucidate the distribution of endogenous E-MAP-115 (ensconsin). Distribution of all GFP-MAP chimeras and endogenous E-MAP-115 (ensconsin) were identical. All show bright fluorescence associated with MTs throughout mitotic progression, independent of which of the two cell types, (TC-7 or MCF-7), which expressed GFP-MAP-chimera, or what level of expression was monitored. (h and m) DAPI staining of the same cells pictured in g and l, respectively. (c) An image of a GFP-EMTB-TC-7 cell expressing a high level of GFP-chimeric protein; note the multipolar spindle, which was common in highly expressing cells (see Table 3). In living cells, mitotic stages were identified only by MT distribution and phase image; in fixed cells, correlation with DAPI stain was used to verify the stage. Bars: in a, 10 μm (for a,b); in c, 10 μm (for c); in d, 10 μm (for d-o).

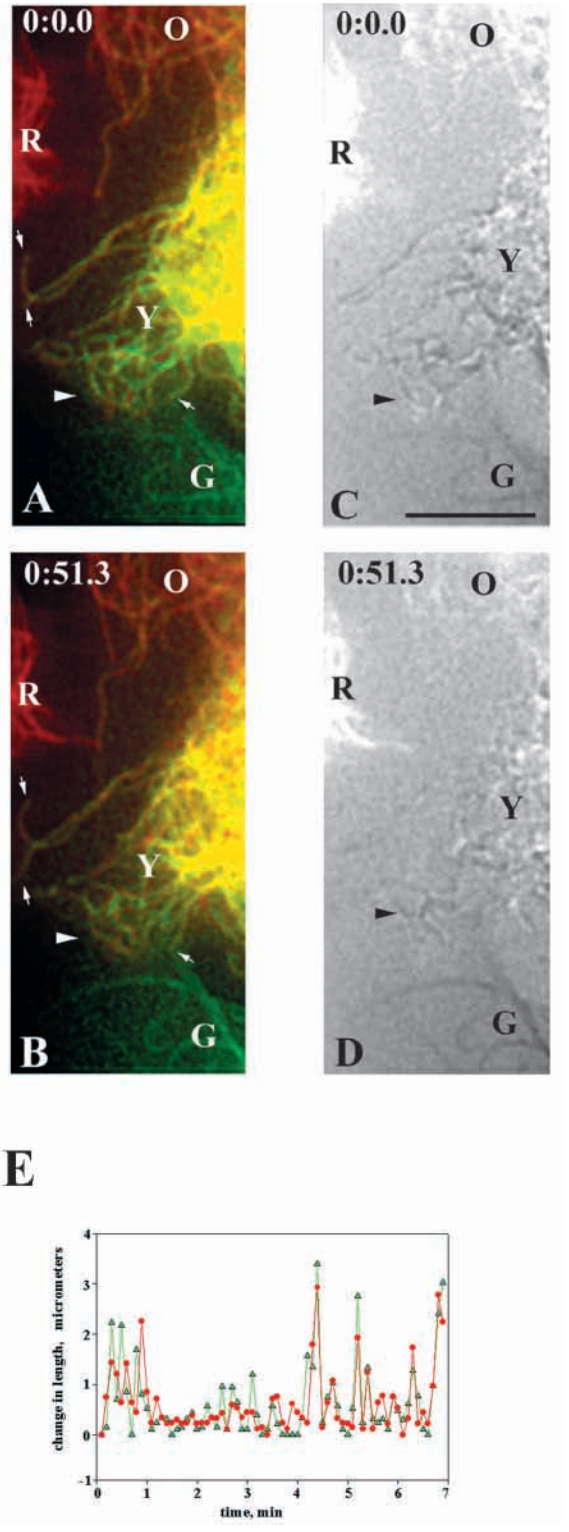

Fig. 6. Dynamic association of GFP-EMTB with MTs during steady-state polymerization/depolymerization. 2×GFP-EMTB-TC-7-L cells whose MTs had been depolymerized with nocodazole (10 μM, 12 hours) were microinjected with X-rhodamine-labeled tubulin. After release from nocodazole (1-3 hours) to allow incorporation of labeled tubulin throughout the MT array, MT growth/shrinkage was observed by time-lapse imaging. Edges of four cells are shown at sample time points: A, C, 0 minutes; B, D, 51.3 seconds after start of the recording. (A and B) X-rhodamine tubulin is red, 2×GFP-EMTB is green, and coincidence of red and green is yellow or orange. (Y), yellow cell expressing 2×GFP-EMTB and microinjected with X-rhodamine tubulin; (O), orange cell expressing a low level of 2×GFP-EMTB and microinjected with X-rhodamine tubulin; (R), red cell with undetectable 2×GFP-EMTB, which has been microinjected with X-rhodamine tubulin, and (G), green cell containing only 2×GFP-EMTB. Arrows (in A,B) mark dynamic MTs in cell Y; whose yellow color indicates that they contain both X-rhodamine tubulin and 2×GFP-EMTB all the way to their ends, whether growing or shrinking. (C and D) GFP images subtracted from corresponding X-rhodamine images. White indicates presence of X-rhodamine but not GFP signal, while black indicates presence of GFP but not X-rhodamine signal. Arrowhead (in A-D) marks MTs in cell Y that may have moved laterally during the 1.5 seconds between capture of red and green images; green and red MT segments in A, B, and black and white ones in C and D, appear to lie subjacent to one another. Otherwise, X-rhodamine and GFP images show perfect correspondence. Bar, 10 μm. (E) Life history plot of a MT end during the time-lapse sequence, monitored with images of X-rhodamine (red line) and GFP (green line). Note that the small differences (<1 μm) in length of ends that can be detected between data from X-rhodamine and GFP fluorescence may represent MT length changes that occurred during the 1.5 seconds that elapsed between capture of the two images. Life history plots, which reflect length changes rather than lateral movements of MTs, quantitatively measure the presence of GFP-MAP chimera at MT tips.

cells (Fig. 7b). Pairwise comparisons of high magnification images in Fig. 7 (compare c,e,g,i, with d,f,h,j) show that, upon inducing polymerization by nocodazole washout, 2×GFP-EMTB fluorescence was observed along the entire length of every MT detectable by X-rhodamine fluorescence. These data demonstrate that, during de novo repolymerization, all MTs bind GFP-MAP chimera essentially concomitant with their polymerization.

E-MAP-115 (ensconsin) does not modulate MT dynamics in vivo

Both E-MAP-115 (ensconsin) and GFP chimeras mimetic of the endogenous MAP are associated with MTs throughout the cell cycle, and we have shown that GFP-MAP chimeras associate with all MTs immediately upon polymerization. From these results, the most likely hypothesis for the MAP's function is that E-MAP-115 (ensconsin) is a modulator of MT dynamics. This hypothesis seemed additionally plausible, for two reasons: First, E-MAP-115 (ensconsin) might be functionally analogous to MAP4, another MAP present on non-neuronal MTs, which has been shown to function as a MT-stabilizing protein in vivo (e.g. Olsen et al., 1995; Nguyen et al., 1999). Second, cells expressing high levels of full-length E-MAP-115 (ensconsin) or its domains (e.g. Masson and Kreis, 1993; also see Table 3) displayed nocodazole-resistant MT bundles, showing that the MAP possesses the capability to stabilize MTs in vivo.

If E-MAP-115 (ensconsin) actually functions as a MT-stabilizing protein in the vivo context, altering MAP expression would be expected to alter MT stability concomitantly. Cells expressing GFP-EMTB chimeras at 4-10 times the level of endogenous MAP do not show bundles of stabilized MTs (Table 3). However, more subtle alterations might be caused by the overexpressed MAP, and these would be observable as alterations in MT dynamics. A careful measurement of MT dynamics in naive TC-7 and those expressing extra MAP

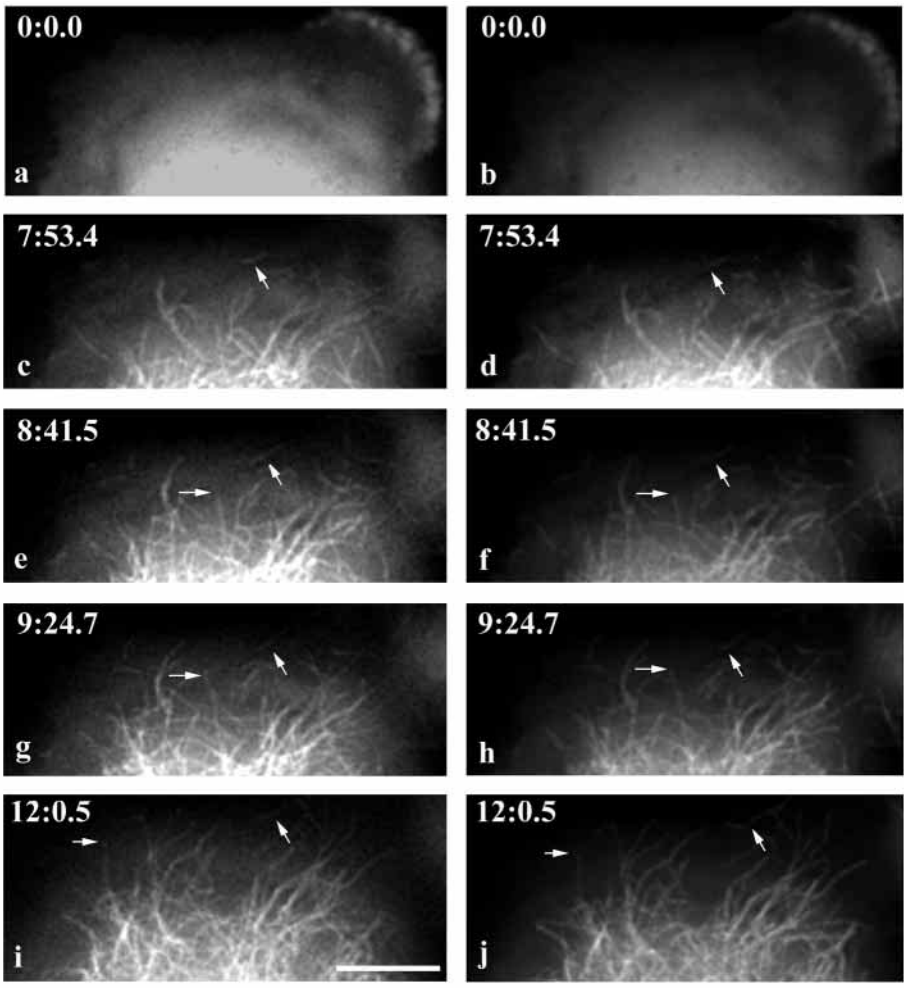

Fig. 7. In vivo polymerization of MTs in 2×GFP-EMTB-TC-7 cells: MAP associates with all MTs immediately upon polymerization. 2×GFP-EMTB-TC-7-L cells grown on coverslips were treated with nocodazole (10 μM, 12 hours) to break down all cellular MTs, then they were microinjected with X-rhodamine-labeled tubulin, incubated a further 1-3 hours, mounted onto a microscope slide and then perfused with nocodazole-free medium to release drug inhibition, allowing regrowth of MTs for the indicated periods of time during dual wavelength digital time-lapse imaging. Fluorescence of 2×GFP-EMTB (a,c,e,g,i) and X-rhodamine tubulin (b,d,f,h,j) on MTs after various intervals of growth: Images depict cells before release from nocodazole (a,b, 0 minutes), and then at a higher magnification, following regrowth for (c,d) 7 minutes 53.4 seconds, and 8 minutes 41.5 seconds, (e,f) 9 minutes 24.7 seconds, and (i,j) 12 minutes, 0.5 seconds. Arrows show single, growing MTs that possess fluorescence from both 2×GFP-EMTB and X-rhodamine tubulin all the way to their ends, indicating rapid association of the MAP molecule with each newly polymerized MT. Bar, 10 μm.

would allow us to demonstrate the MAP's role in modulating MT dynamics; these measurements would also tell us which parameters of MT dynamics are modulated by the MAP.

Accordingly, we made time-lapse recordings of 2×GFP-EMTB-TC-7-L cells and naive TC-7 cells; the former express about ten times more of this MAP than do naive TC-7 cells (Table 2). As shown in the sample in Fig. 8, we quantified the dynamics of about 60 MT ends in ~10 cells of each type. As shown in Table 4, polymerization and depolymerization rates, though variable in magnitude, did not differ significantly between the two cell types. Moreover, the frequency with which MTs underwent rescue or catastrophe events, and the MT dynamicity (Toso et al., 1993) were also equivalent. These data demonstrate that expression of GFP-MAP chimeras, at about ten times the level endogenous to a TC-7 cell (Table 2), does not detectably alter the MT system, including any dynamic parameters. This result strongly contradicts our hypothesis; MT dynamic data suggest that E-MAP-115 (ensconsin) does not normally contribute to MT stabilization in vivo, at least in undifferentiated epithelial cells.

Table 4. Assembly dynamics of MTs in TC-7 cells expressing 2×GFP-EMTB

	Cell line	
Dynamic parameter	2×GFP-EMTB-TC-7-L	Naive TC-7
Growth rate (μm/minute)	4.56±3.61	4.89±3.09
	(P<0.45)	
Shortening rate (μm/minute)	5.08±3.98	5.70±4.27
	(P<0.32)	
Catastrophe frequency (events/minute)	0.34±0.03	0.31±0.02
	(P<0.40)	
Rescue frequency (events/minute)	0.23+0.06	0.27±0.01
	(P<0.37)	
Dynamicity (μm/minute)	2.66±1.35	2.27±1.40
	(P<0.31)	
Cells examined (n=)	11	9
MTs measured (n=)	56	59

All values represent mean ± standard deviation.
Only events of duration ≥0.25 minutes were scored in each cell line.
P values were obtained from the raw data for each MT, using the t-test function (not paired) of SigmaPlot software.

DISCUSSION

Monitoring in vivo distribution and dynamics of GFP-chimeric proteins has enhanced understanding of the functions of numerous cytoskeletal proteins (Ludin and Matus, 1998). We established that GFP conjugates of full-length E-MAP-115 (ensconsin) (GFP-Ensc) or its MT-binding domain (GFP-EMTB), faithfully model MAP behavior in normal, living cells. These constructs allowed us to study MAP function in

vivo, while avoiding artifacts often associated with fixation and staining procedures.

Our experiments addressed important questions à propos of the interaction of E-MAP-115 (ensconsin) with MTs, as well as the MAP's potential to stabilize the MTs to which it binds. First, does this MAP bind to a MT concomitant with, or following, polymerization of a MT? Binding would be expected to depend upon the association/dissociation rate of the MAP with the MT, and also on the size of the pool of unbound MAP in the cell. Our studies showed immediate association of MAP with MTs, either at steady-state (Fig. 6) or during de novo polymerization (Fig. 7). We detected 2×GFP-EMTB along the entire length of all MTs; in contrast, MTs devoid of another MAP, MAP4, all along their length have been documented in immunofluorescence studies of TC-7 and other cells (Chapin and Bulinski, 1994).

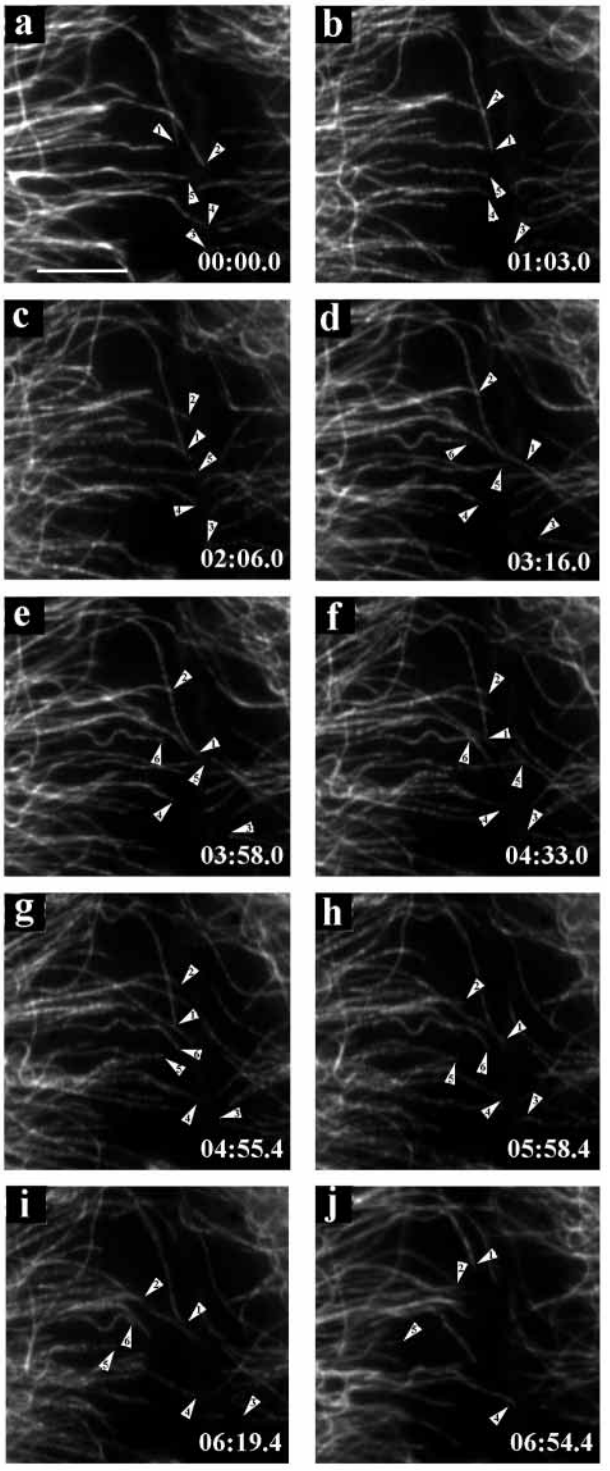

Fig. 8. Microtubules are dynamic in TC-7 cells expressing low levels of 2×GFP-EMTB. MT polymerization was monitored by time-lapse imaging in 2×GFP-EMTB-TC-7-L cells. Each gives the time elapsed since the beginning of the experiment. Numbered arrows denote MTs whose shrinkage/growth was monitored in the experiment; microtubules in peripheral regions of two adjacent cells are shown. For quantification of parameters of MT dynamics, see Table 4.

A second question we addressed is this: Must E-MAP-115 (ensconsin) be stripped from MTs to achieve depolymerization? It was previously proposed that MTs without detectable MAP4 might represent those from which MAP(s) had been stripped prior to depolymerization (Chapin and Bulinski, 1994). Illenberger et al. (1996) purified a kinase they called MARK, which could phosphorylate MAP4 at one or more sites, each sufficient to dissociate it from MTs. Cells transfected with MARK cDNA showed a diminution in the MT array, followed by cell death, prompting Drewes et al. (1997) to conclude that in vivo phosphorylation by MARK removed MAP4 from MTs, destabilizing them such that they depolymerized. In contrast, data we obtained from dual wavelength time lapse imaging demonstrated that removal of E-MAP-115 (ensconsin) from MTs prior to their depolymerization either does not occur in our cells, or it occurs so transiently or locally that we failed to resolve it. Our result does not preclude the possibility that removal of other MAPs, such as MAP4, aids in destabilizing MTs and augmenting depolymerization.

A third question we addressed is the following: Does E-MAP-115 (ensconsin) function as a MT-stabilizing MAP in vivo? In TC-7 cells, we found that all MTs possessed GFP-EMTB chimera at all times, and that the MAP rapidly associated with and dissociated from all MTs. Moreover, comparison of binding of endogenous E-MAP-115 (ensconsin), GFP-Ensc, and GFP-EMTB during the cell cycle in living cells (Figs 1, 3, 5), in lysed cell models (Figs 4, 5), and in cell extracts (data not shown) showed that the MT-binding characteristics of each were indistinguishable, notwithstanding the presence of GFP or of any MAP domain outside of the MT-binding domain, e.g. the C-terminal projection domain. Notably, moderate overexpression of GFP-EMTB did not alter MT dynamic parameters (Table 4), although very high level expression did appear to stabilize MTs, as judged by the facts that (1) GFP-EMTB-TC-7 cells contained bundles of aberrantly stabilized MTs (Table 3), and (2) in a cursory perusal of MT dynamic parameters (i.e. quantification of the dynamics of four MTs in two GFP-EMTB-TC-7 cells) these cells' MTs exhibited almost tenfold lower dynamicity than those in naive TC-7 cells (data not shown). Thus, our data are inconsistent with the proposal that, at physiologically relevant levels, E-MAP-115 (ensconsin) functions as an in vivo regulator of MT stability or dynamics.

Results showing that the level of E-MAP-115 (ensconsin) in undifferentiated cells such as TC-7 or HeLa precludes its action in modulating MT dynamics, contrasts with results of

studies on other MAPs. The other prominent MAP in non-neuronal cells, MAP4, has been shown to exert effects on MT stability when moderately over- (Olsen et al., 1995; Nguyen et al., 1997) or under-expressed (Nguyen et al., 1999), although it should be noted that neither a previous overexpression study (Barlow et al., 1994) nor an immune depletion study (Wang et al., 1996) noted any stability changes in fibroblasts plus or minus normal levels of MAP4. In any case, each of the other cofilamentous MAPs, including MAP1, MAP2, and tau, which associate along the length of the polymer and do not associate with tubulin protomer, have been shown to stabilize MTs in vivo (reviewed by Mandelkow and Mandelkow, 1995). In fact, to our knowledge, ensconsin is the only one of these 'non-motor' MAPs that does not appear to modulate MT dynamics in the in vivo setting. This unique difference suggests that E-MAP-115 (ensconsin) may be functionally distinct from most other MAPs.

It should be noted that Fabré-Jonca et al. (1999) demonstrated increased expression of E-MAP-115 (ensconsin) during differentiation of epithelial cells; it is possible that in terminally differentiated cells the MAP may reach a sufficiently high level to begin to stabilize MTs. It is more likely, however, that the MAP's repertoire of in vivo functions does not include regulation of MT dynamics. Further studies will be required to ascertain E-MAP-115 (ensconsin) functions, for example, functions that may involve cytoskeletal tethering of molecules to MTs, through interaction with the MAP's projection domain.

A major finding reported here, that both GFP-MAP chimeras and endogenous E-MAP-115 (ensconsin) are associated with MTs throughout mitosis, contrasted with behavior previously reported for the endogenous MAP (Masson and Kreis, 1995). We considered potential explanations for this disparity: First, dissociation of endogenous MAP from mitotic MTs had been shown to be temporally correlated with mitosis-specific phosphorylation (Masson and Kreis, 1995); perhaps lack of appropriate phosphorylation of GFP-MAP chimeras prevented them from dissociating from the spindle. However, all three molecules; namely, GFP-Ensc and endogenous E-MAP-115 (ensconsin), which contained the mitosis-specific phosphorylation site; and GFP-EMTB, which did not, remained associated with MTs throughout M-phase. Thus, a deficit in phosphorylation could not readily explain the discrepant results. Disparate results could also arise from cells that differed in MAP level. For example, only a fraction of MAP might dissociate from spindles during mitosis, and this diminution might not be detected in cells with high MAP level. This explanation was ruled out by the fact that cells with all levels of MAP, from transfectants with 10-400 molecules of GFP-MAP chimera per micron of MT (Table 3), to naive cells with 15 molecules of endogenous MAP per micron of MT, all showed continuous association of MAP with mitotic MTs. Thus, the inconsistent results most likely arise from differences in the cell types used. Clearly, in both TC-7 and MCF-7 cells, E-MAP-115 (ensconsin) is continuously bound to MTs throughout M-phase.

Besides important results bearing on potential functions of E-MAP-115 (ensconsin), our study yielded a technical advance in MT imaging. Initial attempts to image GFP-MAP chimeras along single MTs in normal cells proved to be surprisingly difficult, because of insufficient initial fluorescence and significant photobleaching during repeated observation. This situation obtained both in GFP-Ensc-TC-7 and GFP-EMTB-TC-7 cells, even though MT fluorescence was about twice as bright in the latter (transfectants expressed more of the lower mass GFP-EMTB molecule). Time-lapse imaging of fluorescent MTs for extended periods requires excitation illumination and suppression of photobleaching. We found that inhibiting photobleaching by depleting oxygen, though effective for conventional fluorophores, was ineffective for GFP. Thus, only cells with very high GFP-EMTB level (~400 molecules per μm of MT) were amenable to capture of more than 10-20 sequential images. This was a concern because cells with such high levels of GFP-EMTB, whose MAP binding sites on MTs must be saturated (Bulinski and Bossler, 1994), showed phenotypic abnormalities such as bundled MTs and aberrant mitoses (Table 3).

We also predicted that imaging cells with low level expression of GFP-EMTB would be compromised by a second problem, a phenomenon called 'blinking' or 'switching' (Dickson et al., 1997). These investigators showed that illuminated GFP molecules fluoresce for several seconds, cease emission for several more seconds, and then resume fluorescence. After several minutes of this cycle, GFP molecules lose fluorescence. Due to the blinking phenomenon, imaging designed to reveal changes in *distribution* of GFP-EMTB molecules might instead reveal transient or permanent changes in GFP-EMTB *fluorescence*.

For our constructs we used pEGFP-N1, a construct in which wild-type GFP from *Aequorea victoria* (Chalfie et al., 1994) had been mutated at amino acids S65T (Ehrig et al., 1995) and F64L (Cormack et al., 1996) to produce brighter fluorescence and minimal photobleaching. Since we were already using the optimized GFP variant, we increased the fluorescence of individual GFP-EMTB molecules by a means other than mutation; we linked multiple GFP molecules to EMTB. As predicted, cells expressing low levels of 2×, 3×, or 4×GFP-EMTB were amenable to extensive imaging with less profound photobleaching than we had observed in cells expressing (1×)GFP-EMTB. A predicted technical benefit of linking multiple GFP moieties to EMTB is that effects of blinking would be averaged over many GFPs, giving steadier fluorescence intensity during observation.

Thus, the system we developed to study MAP behavior has resulted in a technical advance in imaging MAP, as well as in imaging the MTs to which the MAP binds. Our system satisfies two vital criteria for optimal utilization of GFP conjugates as reporters for endogenous proteins. The first criterion is to establish that the protein's behavior is not altered by the added GFP. This we accomplished by comparing localization and MT-binding properties of GFP-MAP chimeras and endogenous MAP. We demonstrated that the GFP tag did not alter distribution of the MAP during the cell cycle (Fig. 5), and that both endogenous and GFP-chimeric MAP responded identically to extraction by detergent (Fig. 4), or salt (Bulinski et al., 1999; data not shown).

The second criterion our system met was the proof that expression of the GFP-chimera does not alter *cellular* behavior, especially activities in which the proteins of interest; i.e. the MAP or the MTs, play a prominent role. We fulfilled this criterion by showing that MT and mitotic parameters did not differ between 2×GFP-EMTB-TC-7-L and naive TC-7 cells

(Tables 3, 4). In contrast, cells with high levels of GFP-EMTB were perturbed in MT distribution, MT dynamics, and in mitosis (Table 3). It was vital to establish that no subtle alterations in MT dynamics were caused by expression of 2×GFP-EMTB, because substoichiometric concentrations of taxol that do not alter MT polymer level, but do perturb MT dynamics, manifest dramatic effects on cell division (Jordan et al., 1992), and effectively inhibit fibroblast and neuronal growth cone motility (Liao et al., 1995; Tanaka et al., 1995). Thus, demonstrating that parameters of MT dynamics are indistinguishable in 2×GFP-EMTB-TC-7-L and naive cells (Table 4), allowed us to conclude confidently that 2×GFP-EMTB is an authentic reporter for endogenous MAP in cells with phenotypically normal MTs.

In addition to detailed studies of 2×GFP-EMTB-TC-7-L cells, more cursory study of mitotic properties and MT appearance in 3×- and 4×GFP-EMTB-TC-7 cells suggested that these cells are also phenotypically normal. Taken together, our results suggest that hypothesis-driven experiments on E-MAP-115 (ensconsin) have also yielded a technical contribution: We have shown that cells exhibiting low level expression of GFP-EMTB chimeras are amenable to extensive in vivo MT imaging (e.g. Fig. 8), with the confidence that the MTs imaged are not perturbed by the label used to visualize them. Cultures of these cells may be useful for examining influences of various agents on the MAP or the MTs, in populations of living cells in real time.

Our successful use of GFP-EMTB as a non-perturbing label for MTs follows on the heels of several other, more problematic, attempts to use GFP constructs to follow dynamics and movement of cytoskeletal proteins in living cells. Previous investigators found that a GFP tag compromised the function of the cytoskeletal protein to which it was attached. For example, GFP-tagging yeast *tub4p*, a γ-tubulin-related protein, or act1p, yeast actin, did not result in functional complementation of TUB4- or ACT1-null yeast, respectively (Marschall et al., 1996; Doyle and Botstein, 1996). Similarly, in *Dictyostelium discoideum*, actin filaments enriched in GFP-actin did not translocate in a microfilament-sliding assay, apparently because the appended GFP inhibited interaction with the myosin on which the assay depended (Westphal et al., 1996). Clearly, GFP chimeras are not useful as reporters for cytoskeletal proteins if GFP blocks domains vital to functions under study. Our success, in contrast to the cited studies, may be attributable to the fact that GFP-EMTB, like endogenous MAPs, is appended to the MT wall, rather than incorporated into the MT lattice. Alternatively, we may have simply introduced a sufficiently small number of chimeric molecules onto the MT surface (≤150 molecules/μm, or less than four times the level of this MAP in a HeLa cell). In any case, regardless of the ancillary outcome, development of a non-perturbing in vivo label for MTs, experiments described here have answered several questions about MAP behavior, most strikingly that E-MAP-115 (ensconsin) does not function as a MT-stabilizing protein in vivo.

This paper is dedicated to the memory of Dr Thomas Kreis, whose encouragement and stimulating discussions originally prompted our laboratory to return to the study of ensconsin (E-MAP-115; neé 125kD MAP) after a lengthy hiatus. The authors are grateful to Drs Michael Sheetz, Tim Mitchison, Tony Hyman, Helmut Tröster, and David Odde for invigorating discussions, to Pallavi Prasad and Winston Chang for assistance in preparing and characterizing the constructs used, and to Shira Yevin for data analysis. This research was supported by the National Institutes of Health with grants to J.C.B. (CA 70951) and to E.D.S. (GM 24364), and postdoctoral fellowship support to K.F. (AR 08316). C.M.W.-S. was supported by a fellowship from the Jane Coffin Childs Memorial Fund for Cancer Research.

REFERENCES

Barlow, S., Gonzalez-Garay, M. L., West, R. R., Olmsted, J. B. and Cabral F. (1994). Stable expression of heterologous microtubule-associated proteins (MAPs) in Chinese hamster ovary cells: evidence for differing roles of MAPs in microtubule organization. *J. Cell Biol.* **126**, 1017-1029.

Bré, M. H., Pepperkok, R., Hill, A. M., Levilliers, N., Ansorge, W., Stelzer, E. H. and Karsenti, E. (1990). Regulation of microtubule dynamics and nucleation during polarization in MDCK II cells. *J. Cell Biol.* **111**, 3013-3021.

Bulinski, J. C. and Borisy, G. G. (1979). Self-assembly of Hela tubulin and the identification of HeLa microtubule-associated proteins. *Proc. Nat. Acad. Sci. USA* **76**, 293-297.

Bulinski, J. C. and Borisy, G. G. (1980). Microtubule-associated proteins from cultured HeLa cells: Analysis of molecular properties and effects on microtubule polymerization. *J. Biol. Chem.* **255**, 11570-11576.

Bulinski, J. C. and Bossler, A. (1994). Purification and characterization of ensconsin, a novel microtubule stabilizing protein. *J. Cell Sci.* **107,** 2839-2849.

Bulinski, J. C., McGraw, T., Gruber, D., Nguyen, H. L. and Sheetz, M. P. (1997). Overexpression of MAP4 inhibits organelle motility in vivo. *J. Cell Sci.* **110**, 3055-3064.

Bulinski, J. C., Gruber, D., Faire, K., Prasad, P. and Chang, W. (1999). GFP chimeras of E-MAP-115 (ensconsin) domains mimic behavior of the endogenous protein in vitro and in vivo. *Cell Struct. Funct.* (in press).

Chalfie, M., Tu, Y., Euskirchen, G., Ward, W. W. and Prasher, D. C. (1994). Green fluorescent protein as a marker for gene expression. *Science* **263**, 802-805.

Chapin, S. and Bulinski, J. C. (1991a). Non-neuronal 210kD microtubule-associated protein (MAP4) contains a domain homologous to the microtubule-binding domains of neuronal MAP2 and tau. *J. Cell Sci.* **98**, 27-36.

Chapin, S. J. and Bulinski, J. C. (1991b). Preparation and functional assay of tyrosinated and detyrosinated tubulin. *Meth. Enzymol.* **196**, 254-264.

Chapin, S. and Bulinski, J. C. (1994). Cellular microtubules heterogeneous in their content of MAP4 (210Kd MAP). *Cell Motil. Cytoskel.* **27**, 133-149.

Cormack, B. P., Valdivia, R. H. and Falkow, S. (1996). FACS-optimized mutants of the green fluorescent protein (GFP). *Gene* **173**, 33-38.

Dickson, R. M., Cubitt, A. B., Tsien, R. Y. and Moerner, W. E. (1997). On/off blinking and switching behaviour of single molecules of green fluorescent protein. *Nature* **388**, 355-358.

Doyle, T. and Botstein, D. (1996). Movement of yeast cortical actin cytoskeleton visualized in vivo. *Proc. Nat. Acad. Sci. USA* **93**, 3886-3891.

Drewes, G., Ebneth, A., Preuss, U., Mandelkow, E.-M. and Mandelkow, E. (1997). MARK, a novel family of protein kinases that phosphorylate microtubule-associated proteins and trigger microtubule disruption. *Cell* **89**, 297-308.

Ehrig, T., O'Kane, D. J. and Prendergast, F. G. (1995). Green fluorescent protein mutants with altered excitation spectra. *FEBS Lett.* **367**, 163-166.

Fabré-Jonca, N., Allaman, J.-M., Radlgruber, G., Meda, P., Kiss, J. Z., French, L. E. and Masson, D. (1998). The distribution of murine 115-kDa epithelial MT-associated protein (E-MAP-115) during embryogenesis and in adult organs suggests a role in epithelial polarization and differentiation. *Differentiation* **63**, 169-180.

Fabré-Jonca, N., Viard, I., French, L.. E. and Masson, D. (1999). Upregulation and redistribution of E-MAP-115 (epithelial microtubule-associated protein of 115-kDa) in terminally differentiating keratinocytes is coincident with the formation of intercellular contacts. *J. Invest. Dermatol.* **112**, 216-225.

Illenberger, S., Drewes, G., Trinczek, B., Biernat, J., Meyer, H. E., Olmsted, J. B., Mandelkow, E.-M. and Mandelkow, E. (1996). Phosphorylation of microtubule-associated proteins MAP2 and MAP4 by the protein kinase p110^{mark}. *J. Biol. Chem.* **271**, 1-10.

Jordan, M. A., Thrower, D. and Wilson, L. (1992). Effects of vinblastine,

podophyllotoxin and nocodazole on mitotic spindles. Implications for the role of microtubule dynamics in mitosis. *J. Cell Sci.* **102**, 401-416.

Kaech, S., Ludin, B. and Matus, A. (1996). Cytoskeletal plasticity in cells expressing neuronal microtubule-associated proteins. *Neuron* **17**, 1189-1199.

Liao, G., Nagasaki, T. and Gundersen, G. G. (1995). Low concentrations of nocodazole and taxol interfere with fibroblast locomotion without significantly affecting microtubule level: Implications for the role of dynamic microtubules in cell locomotion. *J. Cell Sci.* **108**, 3473-3483.

Ludueña, R. F. (1998). Multiple forms of tubulin: Different gene products and covalent modifications. *Int. Rev. Cytol.* **178**, 207-275.

Ludin, B. and Matus, A. (1998). GFP illuminates the cytoskeleton. *Trends Cell Biol.* **8**, 72-77.

Mandelkow, E. and Mandelkow, E. M. (1995). Microtubules and microtubule-associated proteins. *Curr. Opin. Cell Biol.* **7**, 72-81.

Marschall, L., Jeng, R. L., Mulholland, J. and Stearns, T. (1996). Analysis of Tub4p, a yeast γ-tubulin-like protein: Implications for microtubule-organizing center function. *J. Cell Biol.* **134**, 443-454.

Masson, D. and Kreis, T. E. (1993). Identification and molecular characterization of E-MAP-115, a novel microtubule-associated protein predominantly expressed in epithelial cells. *J. Cell Biol.* **123**, 357-371.

Masson, D. and Kreis, T. E. (1995). Binding of E-MAP-115 to microtubules is regulated by cell cycle dependent phosphorylation. *J. Cell Biol.* **131**, 1015-1024.

Matus, A. (1988). Microtubule-associated proteins: Their potential role in determining neuronal morphology. *Annu. Rev. Neurosci.* **11**, 29-44.

Nguyen, H.-L., Chari, S., Gruber, D. Gruber, Lue, C.-M., Chapin, S. J. and Bulinski, J. C. (1997). Overexpression of full- or partial-length MAP4 stabilizes microtubules and alters cell growth. *J. Cell Sci.* **110**, 281-294.

Nguyen, H. L., Gruber, D. and Bulinski, J. C. (1999). Microtubule-associated protein 4 (MAP4) regulates assembly, protomer-polymer partitioning and synthesis of tubulin in cultured cells. *J. Cell Sci.* **112**, 1813-1824.

Olsen, K. R., McIntosh, J. R. and Olmsted, J. B. (1995). Analysis of MAP4 function in living cells using green fluorescent protein (GFP) chimeras. *J. Cell Biol.* **130**, 639-650.

Pepperkok, R., Bre, M. H., Davoust, J. and Kreis, T. E. (1990). Microtubules are stabilized in confluent epithelial cells but not in fibroblasts. *J. Cell Biol.* **111**, 3003-3012.

Perez, F., Diamantopoulos, G. S., Stalder, R. and Kreis, T. E. (1999). CLIP-170 highlights growing microtubule ends in vivo. *Cell* **96**, 517-527.

Salmon, E. D., Shaw, S. L. Waters, J., Waterman-Storer, C. M., Maddox, P. S., Yeh, E. and Bloom, K. (1998). *Meth. Cell Biol.* **56**, 185-214.

Tanaka, E., Ho, T. and Kirschner, M. W. (1995). The role of microtubule dynamics in growth cone motility and axonal growth. *J. Cell Biol.* **128**, 139-155.

Toso, R. J., Jordan, M. A., Farrell, K. W., Matsumoto, B. and Wilson, L. (1993). Kinetic stabilization of microtubule dynamic instability in vitro by vinblastine. *Biochemistry* **32**, 1285-1293.

Walker, R. A., O'Brien, E. T., Pryer, N. K., Soboeiro, M. F., Voter, W. A., Erickson, H. P. and Salmon, E. D. (1988). Dynamic instability of individual microtubules analyzed by video light microscopy: rate constants and transition frequencies. *J. Cell Biol.* **107**, 1437-1448.

Wang, X. M., Peloquin, J. J., Zhai, Y., Bulinski, J. C. and Borisy, G. G. (1996). Removal of MAP4 from microtubules: Removal of MAP4 from MTs in vivo produces no discernible phenotype at the cellular level. *J. Cell Biol.* **132**, 349-358.

Waterman-Storer, C. M. and Salmon, E. D. (1997). Actomyosin-based retrograde flow of microtubules in the lamella of migrating epithelial cells influences microtubule dynamic instability and turnover and is associated with microtubule breakage and treadmilling. *J. Cell Biol.* **139**, 417-434.

Waterman-Storer, C. M. and Salmon, E. D. (1998a). How microtubules get fluorescent speckles. *Biophys. J.* **75**, 2059-2069.

Waterman-Storer, C. M. and Salmon, E. D. (1998b). Endoplasmic reticulum membrane tubules are distributed by microtubules in living cells using three distinct mechanisms. *Curr. Biol.* **8**, 798-806.

Waterman-Storer, Desai, A., Bulinski, J. C. and Salmon E. D. (1998). Fluorescent speckle imaging: Visualizing the movement, assembly and turnover of macromolecular assemblies in living cells. *Curr. Biol.* **8**, 227-230

Weatherbee, J. A., Luftig, R. B. and Weihing, R. R. (1980). Purification and reconstitution of HeLa microtubules. *Biochemistry* **19**, 4116-4123.

Westphal, M., Jungbluth, A., Heidecker, M., Muhlbauer, B., Heizer, C., Schwartz, J.-M., Marriot, G. and Gerisch, G. (1997). Microfilament dynamics during cell movement and chemotaxis monitored using a GFP-actin fusion protein. *Curr. Biol.* **7**, 176-183.